Apoptosis (2008) 13:364–376
DOI 10.1007/s10495-008-0185-x

ORIGINAL PAPER

Promotion of cell death or neurite outgrowth in PC-12 and N2a cells by the fungal alkaloid militarinone A depends on basal expression of p53

Peter Küenzi · Sabine Kiefer · Anna Koryakina · Matthias Hamburger

Published online: 22 February 2008

Abstract The fungal alkaloid militarinone A (MiliA) was recently found to stimulate neuronal outgrowth in PC-12 cells by persistant activation of pathways that are also involved in NGF-mediated differentiation, namely the PI3-K/PKB and the MEK/ERK pathways. Application of equal concentrations of MiliA to other cells such as the murine neuroblastoma cell line N2a resulted in immediate onset of apoptosis by nuclear translocation of apoptosis inducing factor (AIF), activation of caspases and c-Jun/AP-1 transcription factor without an intermediate differentiated phenotype, although minor transient phosphorylation of PKB and MAPK as well as activation of NF-κB were also observed. Translocation of AIF was preceded by p53 phosphorylation at Ser15 and blocked by pifithrin α, a known inhibitor of p53-transcriptional activity. We here show that both cell types activate the same pathways albeit in different time scales. This is mainly due to contrasting basal expression levels of p53, which in turn regulates expression of AIF. In PC-12 cells, continuous activation of these pathways after prolonged treatment with 40 μM MiliA first led to up-regulation of p53, phosphorylation of p53, release of AIF from mitochondria and its translocation into the nucleus. Additionally, also activation of the c-Jun/AP-1 transcription factor was observed, and PC-12 cells subsequently underwent apoptosis 48–72 h post-treatment. We report that similar pathways working on different levels are able to initially shape very divergent cellular responses.

P. Küenzi · S. Kiefer · A. Koryakina · M. Hamburger (✉)
Institute of Pharmaceutical Biology, University of Basel, Klingelbergstrasse 50, CH-4056 Basel, Switzerland
e-mail: matthias.hamburger@unibas.ch

Keywords Neurite extension · Apoptosis · p53 · AIF · Natural products

Introduction

Neurotrophic factors are capable of preventing apoptosis in neuronal cells, and exogenous supplementation with such factors have been proposed as a new disease-modifying strategy in the treatment of neurogenerative diseases. However, clinical trials have been disappointing so far due to difficulties in delivery of these glycoproteins into the central nervous system [1]. Small non-peptidic molecules with neurotrophic properties, and capable of penetrating the blood–brain barrier, have been proposed as an alternative [2]. In the course of a screening for such molecules we discovered that the fungal alkaloid militarinone A (MiliA) induced neurite extension in PC-12 cells [3]. Due to its amphiphilic properties MiliA was rapidly integrated into the membranous fraction where it triggered PI3-K/PKB- and ERK1/2-dependent differentiation [4, 5]. PKB promotes survival of a variety of neuronal cells and has been shown to be required for neuronal outgrowth [6, 7]. In addition, phosphorylation and activation of the MAPKs ERK1/2 [8] have also been connected with neuronal differentiation [9], albeit its function is not fully clear.

Apoptosis inducing factor (AIF) is a mitochondrial flavoprotein that is mainly located in the mitochondrial intermembrane space. In healthy cells, AIF is required for efficient oxidative phosphorylation. Upon apoptotic insult, it translocates to the cytosol and subsequently into the nucleus where it eventually binds to DNA and induces caspase-independent cell death [10–12]. The concept that AIF is able to induce apoptotic cell death independent of caspases is supported by a series of experiments where

programmed cell death was executed even in presence of chemical caspase inhibitors such as Z-VAD-Fmk (zVAD) or BAF. Moreover, AIF translocation was also observed in mice in the absence of caspase activation [13], and the biochemical changes were consistent with those described in many caspase-dependent cell death models [14]. Contrasting with its death-inducing properties after nuclear translocation, mitochondria-located AIF has been shown to have a protective role in healthy and in tumour cells [11, 15]. Mitochondrial AIF is even thought to contribute to cell survival by protecting cells against harmful oxidative damage in the absence of deleterious stress while predisposing them to a more efficient killing in response to severe stress. Recently, it has been reported that the *aif* gene is a transcriptional target of basal levels of p53 [16].

p53 is a key tumour suppressor protein that is stabilised and phosphorylated due to genotoxic stress and is negatively controlled by Mdm2 which in turn is positively controlled by PI3-K-PKB signalling [17, 18]. Once activated, p53 is able to promote cell-cycle arrest, apoptosis, differentiation, senescence or DNA repair [19, 20]. It may translocate to the nucleus where it regulates a plethora of genes eventually leading to the expression of Bax, Bid, FAS and redox-related genes. Therefore, a model was proposed in which p53 initiates apoptosis through the regulation or generation of reactive oxygen species (ROS) [21].

ROS are by-products of aerobic oxidation, mediate toxicity but also work as signalling molecules [22]. Among others, ROS activate diverse transcription factors such as AP-1, antioxidant responsive element (ARE) and NF-κB [23–25]. AP-1 describes a group of related members of the Jun/Fos family and is involved in various cellular processes depending on the composition of AP-1 dimers and on the cell type. It is commonly thought that in neuronal cells, c-jun has pro-apoptotic function [26], but a simple increase of c-jun concentration was considered to be insufficient to efficiently trigger neuronal cell death [27]. The contribution of AP-1 to survival, apoptosis or differentiation is strictly depending on the cellular situation at a given time point. ARE is important for cell defence under conditions of oxidative stress [24], and NF-κB is a multifunctional transcription factor mainly involved in promoting cell survival [28].

Decline of mitochondrial integrity is considered to be of major importance in generation of oxidative stress and induction of apoptosis through the release of AIF and cytochrome c [14, 29]. It is widely accepted that Bcl-2 proteins such as Bax or Bad are able to disturb the outer mitochondrial membrane leading to the release of these small molecules, and that other Bcl-2 proteins such as Bcl-x_L or Bcl-2 itself are capable to prevent this.

We report here that the small non-peptidic molecule MiliA is capable of inducing signalling complexes such as PI3-K/PKB, MEK/ERK, p53 and accumulation of ROS that together contribute to neurite extension or/and apoptosis depending on the basal expressional level of p53.

Materials and methods

General remark

All experiments have been successfully reproduced at least three times.

Materials and cell culture

Rat PC-12 cells were a kind gift from Prof. Anne Eckert (Neurobiology Research Laboratory, University Clinic for Psychiatry, Basel, Switzerland). Cells were maintained in Dulbecco's modified Eagle medium (DMEM; Sigma-Aldrich, Buchs, Switzerland) supplemented with 5% heat-inactivated foetal calf serum (FCS, Amimed, Basel, Switzerland), 10% heat-inactivated horse serum (Amimed, Basel, Switzerland), 100 U/ml penicillin/streptomycin (Invitrogen, Basel, Switzerland), and 2 mM L-glutamine (Invitrogen, Basel, Switzerland). Murine Neuro 2a (N2a) cells were maintained in DMEM supplemented with 10% FCS, 100 U/ml penicillin/streptomycin and 2 mM L-glutamine. Both cell types were grown in humified atmosphere containing 5% CO_2. PC-12 cells stably overexpressing TrkA were a kind gift from Prof. Frank-D. Böhmer, (Institute of Molecular Cell Biology, Jena, Germany) and were treated as described [3]. The following chemicals have been used: LY294.002, zVAD, pifithrin α (PFTα) (all from Alexis Corporation, Lausen, Switzerland); *N*-Acetyl-L-cysteine (NAC) and nerve growth factor (NGF) (both from Sigma-Aldrich, Buchs, Switzerland). All chemical inhibitors were added 30 min prior to stimulation.

Western blot

Immunoblot analysis was performed according to standard procedures essentially as described [30]. Nitrocellulose membranes were blocked and incubated overnight at 4°C with specific primary Ab diluted in blocking buffer (5% BSA in TBS-Tween): anti-PKB 1:1000; anti-Phospho-PKB (Ser473) 1:1000; anti-ERK1/2 1:2000; anti-Phospho-ERK1/2 (Thr202/Tyr204) 1:1000; anti-AIF 1:2000; anti-Phospho-p53 (Ser15) 1:2000 (all rabbit polyclonal); mouse monoclonal anti-p53 1:1000 (all Cell Signaling Technology, Beverly, MA, USA); goat polyclonal anti-Actin 1:4000 (Santa Cruz Biotechnology, Santa Cruz, CA, USA). Specific bands were tagged using specific, HRP conjugated secondary Abs and detected using the ECL Plus System (GE Healthcare, Little Chalfont, UK).

Immunofluorescence microscopy and light microscopy

PC-12 and N2a cells were fixed in 4% formaldehyde in PBS for a minimal 15 min at 4°C, permabilised with 0.2% Triton-X (prepared in PBS containing 10% heat-inactivated FCS) and then incubated with primary Ab. The Abs were diluted in PBS containing 10% heat-inactivated FCS and used at the following conditions: rabbit polyclonal anti-AIF (diluted 1:50), rabbit anti-Phospho-p53 (Ser15) (diluted 1:100), mouse monoclonal anti-p53 (diluted 1:200) (all from Cell Signaling CST). Subsequently the cells were washed thrice with PBS and incubated for 1 h with affinity-purified Alexa-Fluor 488 goat anti-rabbit IgG (H + L) or Alexa-Fluor 488 goat anti-mouse IgG (H + L) (both from Invitrogen-Molecular Probes, Basel, Switzerland), respectively. Nuclei were counterstained with Dapi (diluted 1:4000 in PBS) (from Invitrogen-Molecular Probes, Basel, Switzerland). Cells plated on coverslips were mounted on glass slides and visualised by confocal microscopy (Leica DM RXE scanning confocal microscope) using Leica confocal software, version 2.5 (Leica Microsystems, Heidelberg, Germany) or on a fluorescence microscope (Axiophot, Carl Zeiss AG, Jena, Germany) using the analySIS Software (Soft Imaging Systems, Münster, Germany). Identical exposure times were used across conditions.

Light microscopy pictures were taken on a Leitz Laborlux (Ernst Leitz, Wetzlar, Germany) equipped with a Leica DC200 Camera (Leitz Microsystems AG, Glattbrugg, Switzerland) and analysed with Leica DC Viewer Software version 3,2,0,0 (Leica Microsystems AG, Heerbrugg, Switzerland).

Flow cytometry and measurement of membrane potential

To detect caspase activation, staining with FITC-valyl-alanyl-aspartic acid fluoromethyl ketone (FITC-VAD-fmk; Promega) was carried out as described [30]. Annexin V staining of exposed membrane phosphatidylserine was carried out using the Annexin V assay kit (Roche Diagnostics, Rotkreuz, Switzerland) following the manufacturer's protocol. Quantification of loss of membrane potential was determined by incubating 1×10^6 cells with 2 nM $DiOC_6(3)$ in serum-reduced media at 37°C for 30 min. After start of treatment, aliquots were taken at time points indicated, diluted in PBS and subjected to flow cytometry. FACS Analysis was performed on a Dako CyAn™ ADP LX 7 using Summit software (DakoCytomation, Fort Collins, CO, USA).

Measurement of intracellular ROS

The accumulation of ROS in PC-12 and N2a cells was determined by analysis of dichlorofluorescein fluorescence. Cells were plated in serum-containing DMEM into 96-well plates and allowed to adhere overnight at 37°C. After washing twice with PBS, 2,7-dichlorofluorescein diacetate (DCFH-DA; Invitrogen-Molecular Probes, Basel, Switzerland) was applied at 10 μM in PBS for 45 min at 37°C. After removal of the supernatant, cells were re-suspended in serum-containing DMEM including drugs or vehicle only and incubated for 60 min at 37°C. DCF fluorescence was quantified (excitation: 492 nm; emission: 535 nm) using a Chameleon microplate reader (Hidex Oy, Turku, Finland).

Alternatively, cells were left to grow on coverslips and subsequently loaded with 5 μM DCFH-DA for 30 min. After incubation with drugs in serum-containing DMEM, the cells were fixed with MeOH at −20°C for 5 min and analysed by immunofluorescence microscopy as described above. Identical exposure times were used across conditions.

Preparation of nuclear extracts, electrophoretic mobility shift assay and supershift

Cells were collected and washed with ice-cold PBS (pH 7.4) and lysed in a hypotonic buffer (10 mM Hepes, pH 7.9, 60 mM KCl, 1 mM EDTA, 1 mM DTT, 0.5% NP-40) containing protease inhibitors (1 mM PMSF, 1× Complete® Protease Inhibitors (Roche Diagnostics, Rotkreuz, Switzerland)). The nuclei were collected by centrifugation at 800*g* for 5 min at 4°C and washed once in ice-cold hypotonic buffer without NP-40. Nuclei were subsequently re-suspended in nuclear buffer (250 mM Tris–HCl, pH 7.8, 60 mM KCl, 1 mM EDTA, 1 mM DTT, 0.5% NP-40) containing protease inhibitors (1 mM PMSF, 1× Complete® Protease Inhibitors). Nuclear membranes were disrupted by freeze-thawing followed by centrifugation at 13,200*g* for 30 min. The supernatant (nuclear extract) was collected and the protein concentration was measured using Coomassie® Protein Assay Reagent (Sigma-Aldrich, Buchs, Switzerland). The binding reactions were carried out as described [31]. Briefly, nuclear extracts containing 3 μg nuclear proteins were incubated for 20 min with ^{32}P-radiolabelled oligonucleotides in 20 μl reaction buffer. For supershift analysis, 1 μg of anti-c-jun (Santa Cruz Biotechnology, Santa Cruz, CA, USA) was added and incubated on ice for another 30 min. Nuclear protein-oligonucleotide and antibody-protein-oligonucleotide complexes, respectively, were resolved by electrophoresis on a 4% non-denaturing polyacrylamide gel in 0.25× TBE buffer at 20 V/cm for 35 min at room temperature. The gel was dried and autoradiographed on an intensifying screen at −80°C. Double stranded, palindromic oligonucleotides containing the consensus sequences for ARE (5′-AAA TGG CAT TGC TAA TGG TGA CAA AGC AAC T-3′) [32], NF-κB (5′-AGT

TGA GGG GAC TTT CCC AGG C-3′) [31] or AP-1 (5′-GAA TCG AGC ATG AGT CAG ACA CA-3′) [33] were used.

Results

We previously reported [3] that addition of 40 μM MiliA to PC-12 cells for 24 h after pre-treatment with NGF [34] induced neurite outgrowth which was attributed to the NGF-dependent up-regulation of its receptor TrkA. However, pre-treatment with a commercially available TrkA-inhibitor that was able to prevent NGF-induced phosphorylation of PKB and MAPKs, did not prevent MiliA-dependent phosphorylation of these proteins (Fig. 1a) and suggested that phosphorylation of TrkA was not involved in MiliA-induced neurite extension. When applying 40 μM MiliA to PC-12 cells stably over-expressing TrkA (TA) and naïve PC-12, we observed similar neuronal outgrowth in both cases (Fig. 1 and [3]. In addition, phosphorylation of PKB and MAPKs in TA (not shown) and naïve PC-12 was found (Fig. 1c).

Since up-regulation of the PKB and MAPK-pathways was independent of TrkA, we wanted to know if MiliA-induced phosphorylation of these signalling molecules occurred also in other neuronal cell-lines. Treatment of N2a cells with 40 μM MiliA led to a down-regulation of the endogenous PKB and MAPK phosphorylation (Fig. 1 e). This was accompanied by a marked loss of protein content from samples treated with MiliA compared to vehicle-treated controls (not shown). Moreover, light microscopy revealed that most of the cells had lost adherence, were oddly shaped or had crumbled (Fig. 1d).

To discriminate between necrotic and apoptotic cell death, we double-stained N2a cells treated with 40 μM MiliA or vehicle only with Annexin V/PI. The overwhelming part of cell death observed was due to apoptotic mechanisms (Fig. 2a) becoming evident as early as 2 h post-treatment. Additionally, chromatin condensation

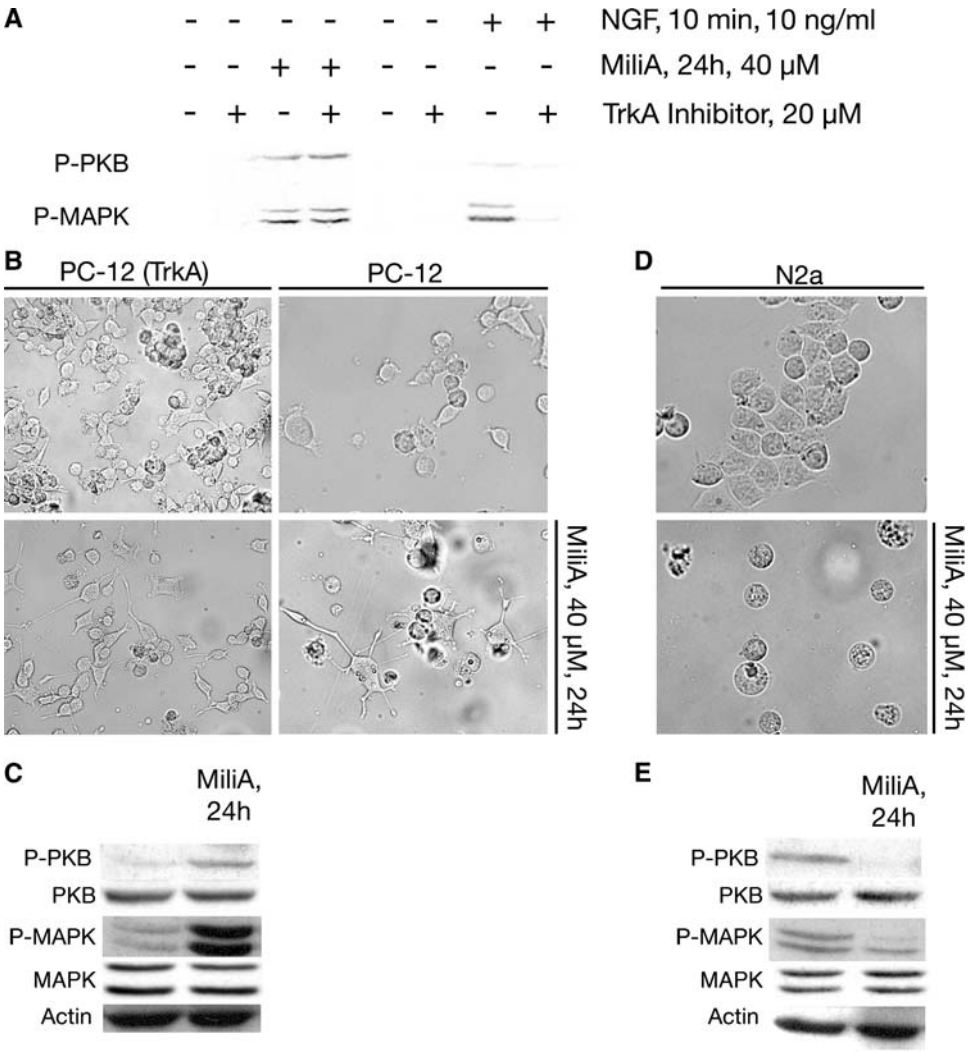

Fig. 1 40 μM MiliA induced TrkA-independent neurite extension in PC-12, but immediate apoptosis in N2a cells. (**a**) Inhibition of TrkA blocked NGF-dependent but not MiliA-dependent phophorylation of PKB and ERk1/2. (**b**) PC-12 cells stably transfected with TrkA (left panels) and naïve PC-12 (right panels) showed similar neuronal outgrowth after 24-h treatment with MiliA. (**c**) Phosphorylation of PKB (Ser473) and MAPKs (ERK1/2; Thr202/Tyr204) was clearly detected after 24 h in PC-12 cells. (**d**) N2a cells lost adherence and normal shape upon addition of MiliA and (**e**) no additional phosphorylation of PKB (Ser473) nor MAPKs (Thr202/Tyr204) could be detected after 24 h

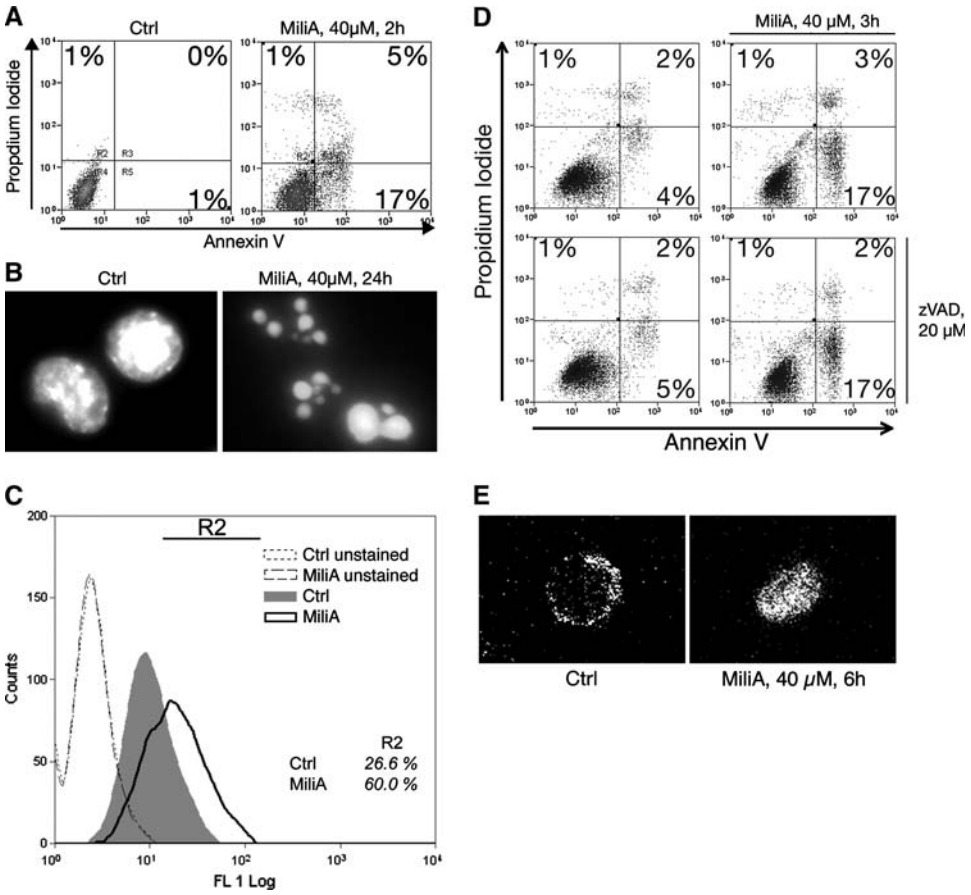

Fig. 2 Treatment with 40 μM MiliA led to caspase-dependent as well as -independent apoptosis in N2a cells. (**a**) Early signs of apoptosis by binding of Annexin V to the cell surface were detected as early as 2 h after treatment with MiliA (40 μM). (**b**) Late signs for programmed cell death such as chromatin condensation were observed in cultures treated with 40 μM MiliA for 24 h. (**c**) General activation of caspases was detected by FACS analysis of FITC-VAD-Fmk-stained cells after 24 h. (**d**) Co-treatment with the general caspase inhibitor zVAD (20 μM) led to only a marginal reduction of programmed cell death after 3 h as shown by Annexin V/PI staining. (**e**) Release and nuclear translocation of AIF was observed in cells treated for 4 h or longer, as shown by confocal immunofluorescence analysis

occurred in cells treated with MiliA for 8 h or longer (Fig. 2b), as visualised in N2a cells stained with Dapi. To test if caspases were involved in the execution of the cellular death observed, MiliA-treated N2a cells were stained with the FITC tagged form of the general caspase inhibitor zVAD and submitted to FACS-analysis: A distinct population showing activation of caspases roughly doubled from 26.6 to 60% 24 h post-treatment (Fig. 2c). We tested in a next step whether pre-treatment with zVAD (20 μM) would be able to suppress onset of apoptosis, but addition of zVAD only slightly diminished the extent of Annexin V-positive cells by $-2.3 \pm 8.7\%$ (data calculated from six independent experiments), and a complete inhibition was never observed after 3 h of treatment with 40 μM MiliA (Fig. 2d). Besides, co-incubation of N2a cells with zVAD and MiliA did not slow the progress of apoptosis, and a phenotype showing neurite extension was observed neither in absence nor in presence of zVAD. As caspase-independent pathways could in addition be activated by administration of MiliA, we checked for nuclear translocation of AIF, a protein normally residing in the mitochondrial intermembrane space [10]. In N2a cells, AIF translocation was detected by confocal immunofluorescence microscopy as early as 4–6 h post-treatment (Fig. 2e). When we checked for simultaneous release of cytochrome c, another pro-apoptotic mitochondrial protein [35], we failed to detect any significant change in localisation (not shown). These findings suggested a specific release of AIF.

As PC-12 showed neurite extension 1 day after addition of 40 μM MiliA, we investigated the effect of prolonged MiliA-treatment on PC-12 cells. Treatment for 1 day only slightly elevated the quantity of Annexin V-positive and Annexin V/PI double-positive cells, but these numbers were substantially increasing after 3 days (Fig. 3a). However, also PI-positive cells were observed and suggested additional necrotic mechanisms. Next we looked for caspase-activation using FACS-analysis of FITC-VAD-Fmk-stained cells but failed to detect any activation 1 day post-treatment (Fig. 3b). Even after 2 days post-treatment, no activation was observed (not shown). However, most of cells showed clear nuclear translocation of AIF between 2 and 3 days post-treatment (Fig. 3c) and analogous to the situation in N2a cells, no significant change in cytochrome c localisation could be detected.

Militarinone A has been reported to rapidly integrate into the membranous fraction [3] due to its amphiphilic properties [36], whereas release into the cytoplasm was markedly slower. As both PC-12 and N2a cells showed release of AIF, we isolated whole, viable mitochondria

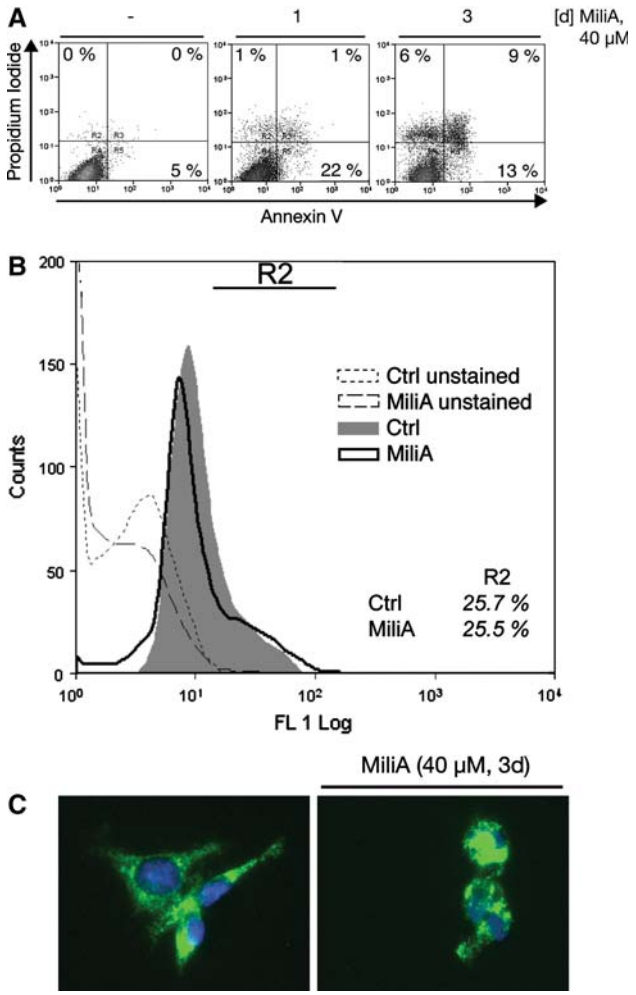

Fig. 3 PC-12 cells undergo homologous apoptosis as N2a cells upon prolonged treatment with 40 µM MiliA. (**a**) Early signs for apoptosis were detected after 1 day and became more pronounced after 3 days, as shown by binding of Annexin V to the cell surface and FACS Analysis in PC-12 cells. (**b**) General activation of caspases was not detected by FACS analysis of FITC-VAD-Fmk stained cells after 1 day. (**c**) Translocation of AIF (green) into the nucleus (blue) in PC-12 cells after a 3 day-treatment with MiliA (40 µM)

from both cell lines to check for membranal integration of MiliA. This rapidly occurred between 30 and 120 s after addition of the compound and was indistinguishable from integration into the cellular membrane (not shown) in both cell types. This observation was unexpected given that N2a showed release of AIF and early apoptosis whereas PC-12 displayed neurite outgrowth and a late onset of cell death. As loss of membrane potential is a sign for the de-stabilisation of mitochondria and a pre-requirement for AIF-release [37], we expected to see a rapid depolarisation in N2a, and a significantly slower effect in PC-12. Loss of membrane potential, however, took place at comparable speed in both cell lines (Fig. 4a). We therefore postulated that PC-12 cells would notwithstanding be less prone to the release of ROS from mitochondria due to loss of membrane potential and we visualised the occurrence of ROS-derived oxidation by measurement of DCF fluorescence via immunofluorescence microscopy. But again, both cell lines reacted in a similar manner to the administration of MiliA (Fig. 4b). When we quantitatively measured the production of ROS we found no significant difference between PC-12 and N2a cells (Fig. 4c). Moreover, the production of ROS by 40 µM MiliA was comparable to administration of 100 µM H_2O_2 and could be efficiently blocked by addition of 15 mM NAC. Given the fact that between depolarisation of the mitochondria and release of ROS, respectively, and induction of cellular death passed several hours (N2a) or even 1–3 days (PC-12), we assume that the release of ROS resulted in activation of signalling pathways not directly involved in apoptosis, as suggested by other publications [38].

To test the involvement of ROS-production in the propagation of apoptosis and neurite extension, respectively, we co-treated both cell-lines with 40 µM MiliA and 15 mM NAC. PC-12 cells remained unaffected (not shown) and N2a cells showed an apoptotic phenotype indistinguishable from MiliA-only treated cells (Fig. 4d). Even though NAC blocked accumulation of ROS (Fig. 4c), the compound did not rescue N2a cells from cell death.

Neither loss of membrane potential nor increase of ROS-levels sufficiently explained the marked difference in reaction of PC-12 and N2a cells to MiliA treatment. Therefore we tested for DNA-binding activities of transcription factors that are reportedly activated by ROS, and bind to consensus sequences of ARE, NF-κB and AP-1 [23–25]. ARE activity raised rapidly and transiently in N2a and PC-12 after addition of MiliA, reaching its peak after 1 h (Fig. 5a) as shown by electrophoretic mobility shift assay (EMSA). DNA-binding activity of AP-1 (Fig. 5b) and NF-κB (Fig. 5c), on the other hand, were differentially regulated in the two cell lines. N2a showed rapid induction of NF-κB and AP-1-binding, peaking between 2 and 4 h. Thereafter, no further activity could be detected. In PC-12 cells, binding of these two transcription factors was more pronounced but only observed from 24–48 h post-treatment.

To test if AP-1 and NF-κB were activated by ROS, we incubated N2a and PC-12 cells pre-treated with 15 mM NAC with MiliA for 4 and 24 h, respectively, and performed EMSA. Only the NF-κB DNA-binding activity was successfully inhibited by NAC in both cell lines (Fig. 5d), whereas AP-1 remained unaffected (not shown). These experiments suggested that ROS would not directly be involved in MiliA-dependent apoptosis but could contribute to initial survival mechanisms mainly through NF-κB activation.

p53 plays an important role in the management of intracellular stress and regulates basal levels of AIF [16].

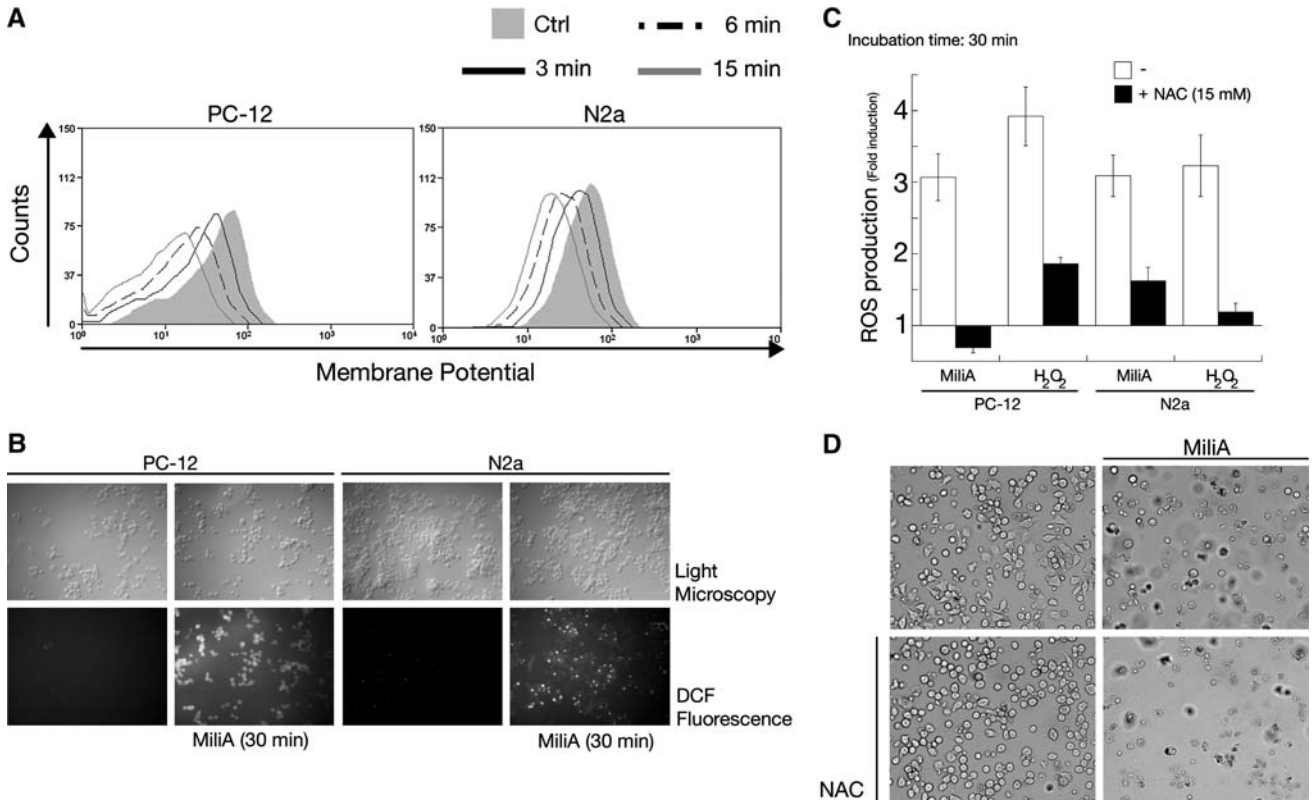

Fig. 4 Immediate loss of membrane potential and release of ROS were detected in both cell lines after addition of 40 μM MiliA. (**a**) Loss of membrane potential was observed shortly after addition of MiliA in PC-12 and N2a. (**b**) ROS production in both cell lines, as shown by immunofluorescence analysis of DCF. (**c**) Production of ROS quantitatively measured by DCF fluorescence in a multiplate reader. Data shown were calculated from three independent experiments and normalised to untreated cells. (**d**) N2a cells treated with 40 μM MiliA overnight underwent apoptosis and were not rescued by addition of NAC (15 mM)

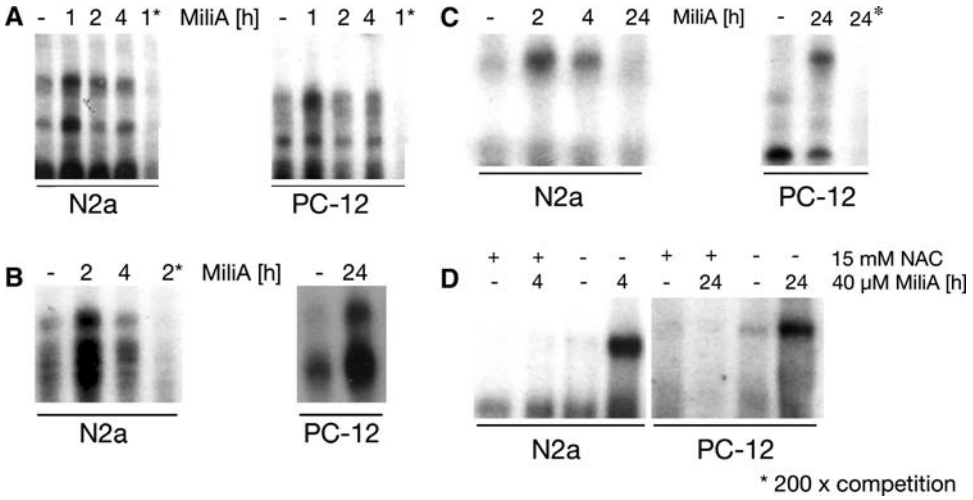

Fig. 5 Activation of the ARE, AP-1 and NF-κB transcription factors after addition of 40 μM MiliA in both cell lines as revealed by EMSA. DNA-binding activity of NF-κB was completely abolished by addition of 15 mM NAC. (**a**) Increased transient binding to the ARE consensus sequence was observed as early as 1 h post-treatment that declined thereafter. There was no obvious difference in ARE DNA-binding activity between PC-12 and N2a cells. (**b**) AP-1 and (**c**) NF-κB were transiently activated in N2a cells peaking at around 2 h post-treatment. PC-12 cells on the other hand showed more persistant DNA-binding activities that began 24 h after start of treatment.(**d**) Addition of 15 mM NAC completely inhibited MiliA-dependent NF-κB DNA-binding activity in both cell lines

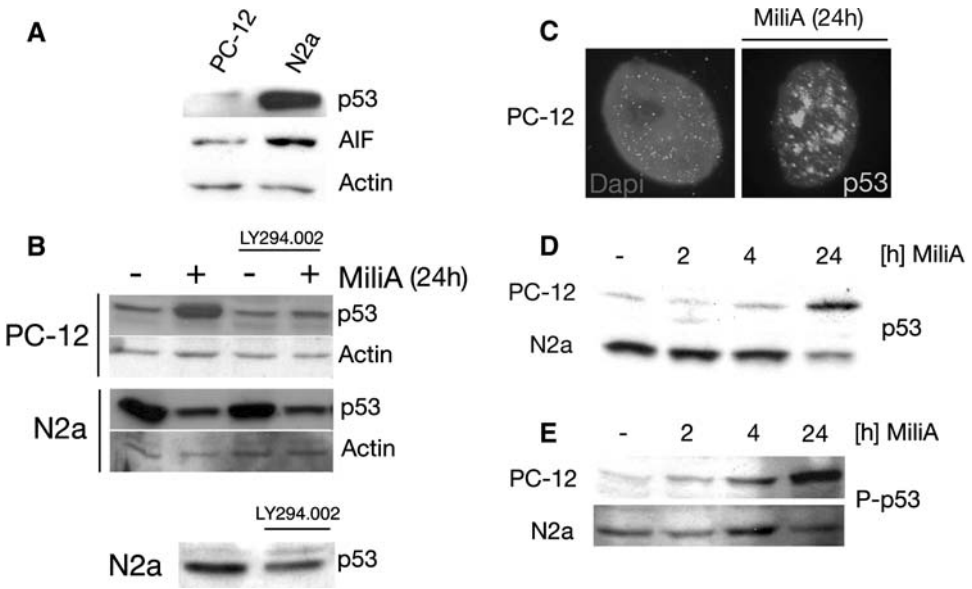

Fig. 6 N2a showed higher expression of p53 and AIF compared to PC-12 cells, and stabilisation of p53 was positively regulated by PI3-K. (**a**) Protein levels of p53 and AIF were higher in N2a than in PC-12 cells. (**b**) Co-treatment with 50 μM LY294.002 efficiently inhibited MiliA-dependent stabilisation (40 μM, 24 h) of p53 in PC-12 but did not block down-regulation in N2a cells. It did, however, slightly diminish basal expression of p53 in N2a cells. (**c**) p53 was almost exclusively localised in the nucleus of PC-12 cells before and after treatment with MiliA for 24 h (40 μM). (**d**) MiliA-dependent down-regulation of p53 in N2a cells did not take place before 4 h post-treatment. (**e**) Phosphorylation of p53 at Ser15 in response to treatment with MiliA (40 μM)

AIF appears to play a dual role: it protects cells against oxidative damage when located in the mitochondria, but increases the chance to succumb to cell death in response to severe stress and subsequent translocation of AIF. As there was a distinct release and nuclear translocation of AIF in both cell lines after addition of 40 μM MiliA, we analysed the expression of p53. N2a cells showed a high basal expression of p53 compared to PC-12 cells and a higher expression of AIF (Fig. 6a). Treatment of PC-12 with MiliA lead to up-regulation of p53, which was almost exclusively localised in the nucleus, whereas N2a cells showed a down-regulation 24 h post-treatment (Fig. 6b, c). The stabilisation of p53 in PC-12 cells was unexpected, since concommittant activation of PKB occurred (Fig. 1c). PKB has been reported to negatively regulate p53 through Mdm2 [17]. We, however, found that phosphorylation of PKB positively regulated p53, as co-treatment with LY294.002, a PI3-K-inhibitor, efficiently blocked PKB phosphorylation and stabilisation of p53 (Fig. 6b). A similar finding was previously published for p53 activation by cisplatin that was equally blocked by the PI3-K-inhibitor [39]. LY294.002, however, did not interfere with the MiliA-dependent down-regulation but led to a slightly diminished expression of basal p53 in untreated N2a cells after incubation with LY294.002 for 1 day (Fig. 6b).

As we had suggested that high p53 expression in N2a cells might be responsible for the sensitisation towards apoptosis induced by MiliA, it was surprising to find p53 down-regulation after 24 h in N2a. However, this down-regulation only occurred after induction of apoptosis. A time course experiment of p53 expression did neither show up- nor down-regulation within 4 h post-treatment (Fig. 6 d). To analyse activation of p53, we used an antibody directed against the phosphorylated form of p53 (Ser15), which was shown to be essential for its pro-apoptotic activity [40, 41]. We, however, only found a significant increase 4 h after addition of 40 μM MiliA, essentially before AIF translocation was observed (Figs. 6e and 2e). In PC-12 cells, stabilisation and activation by phosphorylation of p53 was not observed before 24 h post-treatment, but well before translocation of AIF could be detected (Figs. 6e and 3c).

To check if activation of p53 was indeed responsible for release of AIF and its nuclear translocation, we added MiliA to cells pre-treated for 30 min with PFTα, a known inhibitor of p53-transcriptional activity [42]. Consequently, localisation of AIF remained unchanged in PFTα pre-treated cells upon administration of MiliA in both cell types after 6 h (N2a; Fig. 7a) and 3 days (PC-12; Fig. 7c), respectively. Further, we checked if induction of apoptosis could be blocked by pre-treatment with PFTα and/or PFTα/zVAD combined treatment, which in fact was the case: PFTα alone or in combination with zVAD efficiently blocked initiation of apoptosis as measured by FACS of Annexin V/PI-double stained cells in both N2a (Fig. 7b) and PC-12 cells (Fig. 7d). zVAD (20 μM) alone, however,

only showed marginal reduction of Annexin V-positive cells in N2a and no reduction in PC-12. This is in agreement with the finding that PC-12 showed no caspase-activation in our assays in response to MiliA (Fig. 3b). Even application of up to 100 μM zVAD did not block onset of programmed cell death in neither cell line (not shown).

As LY294.002 blocked stabilisation of p53, we tested if treatment with the inhibitor 30 min prior to addition of MiliA would reduce the extent of cell death in N2a. Co-treatment with LY294.002 efficiently inhibited binding of Annexin-V after 3 h, and only a fraction of the cells lost their shape and adherence after 24 h (Fig. 8a, b).

As treatment with LY294.002 slightly reduced basal levels of p53 in N2a cells (Fig. 6b), we investigated whether phosphorylation at Ser15 of p53 would be repressed as well. Use of an antibody directed against P-p53 in immunofluorescence microscopy showed that activation of p53 by 40 μM MiliA was indeed affected by pre-treatment with LY294.002 (Fig. 8c). 95.5 ± 4.1% of MiliA-treated cells showed phosphorylation of p53 in immunofluorescence microscopy vs. 55.2 ± 4.2% in MiliA/LY294.002 co-treated cells (data calculated from three independent experiments). This reduction was confirmed by analysis of protein samples by SDS-PAGE (Fig. 8d) and was obviously sufficient to prevent immediate onset of apoptosis. However, MiliA-treated N2a cells in presence of LY294.002 succumbed to cell death between 24 and 48 h post-treatment (not shown).

Given that pre-treatment with LY294.002 prolonged survival of MiliA-treated N2a cells, we also applied the PI3-K-inhibitor to PC-12 cells to see if neurite extension and/or late apoptosis would be inhibited. However, PC-12 cells died within 24 h after addition of 50 μM LY294.002 in presence, but also in absence of 40 μM MiliA (not shown). Therefore we continued with N2a cells and observed postponed MiliA-dependent activation of the AP-1 transcription factor in presence of LY294.002 24 h after start of treatment. Interestingly, DNA-binding activity of AP-1 was not detected in MiliA-only treated cells at this time point (Figs. 9a and 5b). MiliA-dependent NF-κB DNA-binding activity on the other hand remained unchanged in presence or absence of LY294.002 (Fig. 5c and not shown). We therefore tested the hypothesis, that raised AP-1 DNA-binding activity is a pro-apoptotic event in this context [43]. As binding of c-jun to AP-1 consensus sequences is considered to be pro-apoptotic [26], we performed supershift analysis using a specific antibody directed against c-jun. We found c-jun-binding in both in MiliA-treated N2a after 4 h as well as in PC-12 after 24 h (Fig. 9b). In addition, the same supershift was also observed in N2a cells co-treated with LY294.002 and MiliA after 24 h (not shown).

Discussion

In this study we present evidence that a simple molecule by activating identical pathways is able to trigger events as diverse as neurite extension and apoptosis.

Differentiation is a complex process and involves diverse signalling pathways. In PC-12 cells, neuronal differentiation is usually initiated by the binding of NGF to TrkA and involves the subsequent activation of PI3-K/PKB, PKCs, Ras and MEK/ERK [5]. MiliA, a pyridone alkaloid from *Paecilomyces militaris* [36] basically does the same: it activates PKB and ERK1/2 [3] but circumvents the need for TrkA. This results in neurite extension in PC-12, and apoptosis in N2a cells. The outcome is similar to that reported for geldanamycin, an Hsp90 inhibitor, which provoked programmed cell death in PC-12 and neurite extension in N2a cells [44]. In another study using a MiliA-related compound, (+)-*N*-Deoxymilitarinone A, cytotoxic effects were observed in the human neuroblastoma cell line IMR-32, and neurite extension in PC-12 cells [45].

We report that MiliA is capable of initially driving two basically independent signalling pathways. First, it provides NGF-like activity, leading to neurite extension. The mechanism for activation of PI3-K/PKB and MEK/ERK1/2, however, remains elusive. As MiliA showed high affinity for membraneous compartments, we investigated possible stimulation of the small G-proteins Ras and Rac which are activated at the cytoplasmic side of the cellular membrane [9, 46, 47] but could not detect any consisting and specific activation neither at early nor late time points (data not shown).

By additional insertion into mitochondrial membranes, MiliA disturbed their integrity, which resulted in loss of membrane potential, release and accumulation of ROS, in both cell lines at comparable speed. Since addition of NAC blocked increase of ROS in PC-12 and N2a, but not the apoptotic pace, we assume that the release of oxidative molecules from mitochondria did not trigger apoptosis by itself. Furthermore, NAC did not inhibit cellular death in N2a and blocked NF-κB-activation suggested that accumulation of ROS was involved in defence and survival mechanisms. The subsequent release of AIF and its translocation to the nucleus was fast in N2a but delayed in PC-12, and suggests involvement of additional elements that control release of molecules at mitochondrial level [48]. This was corroborated by the fact that we were unable to detect co-release of cytochrome C. How exactly MiliA induces loss of membrane potential, a necessary pre-requisite for subsequent release of AIF [37], needs further investigation.

Second, it activates p53-dependent apoptosis [19, 20] mainly through a caspase-independent mechanism involving nuclear translocation of AIF, a molecule that is

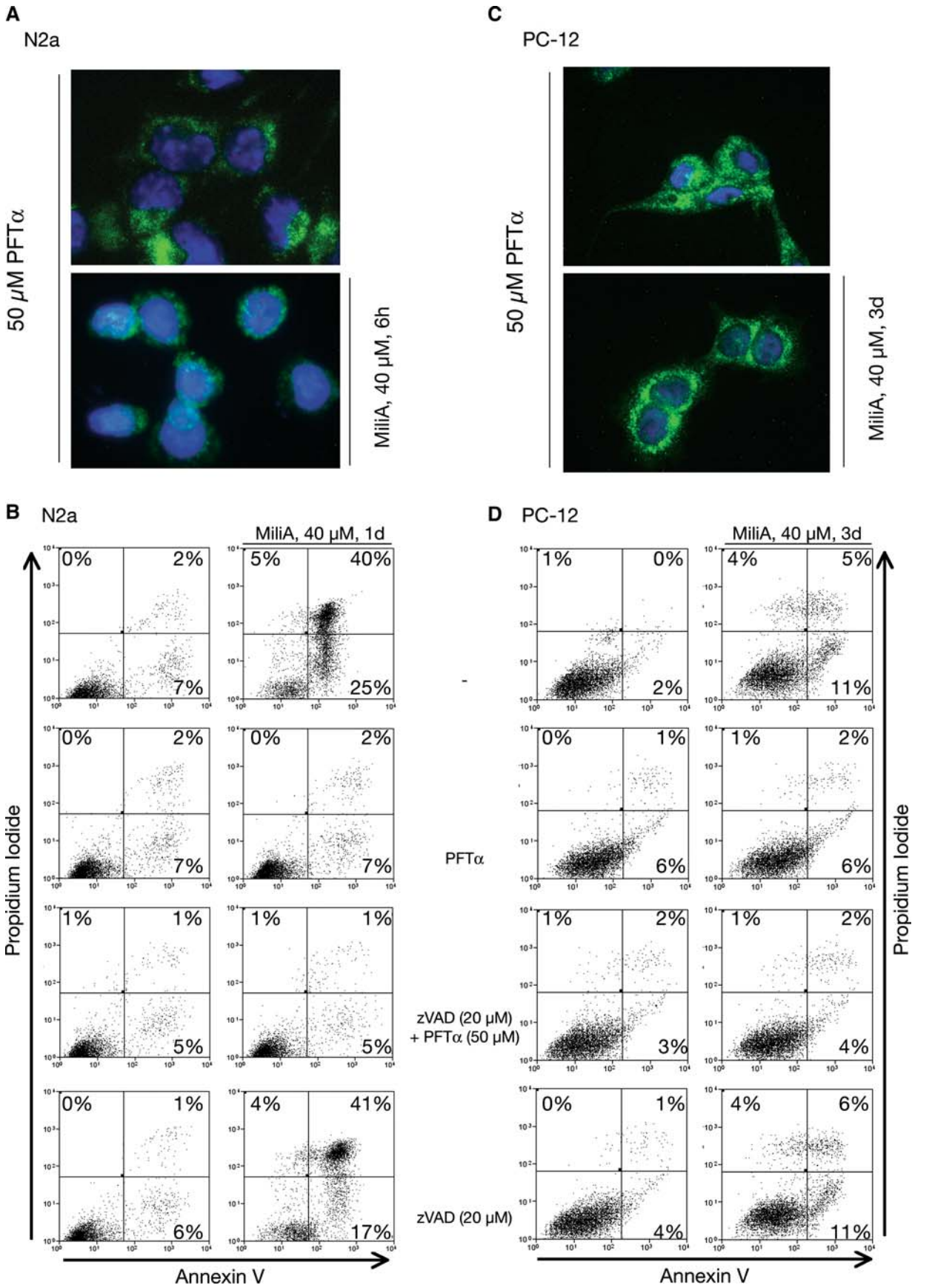
A
N2a
50 μM PFTα
MiliA, 40 μM, 6h
C
PC-12
50 μM PFTα
MiliA, 40 μM, 3d
B
N2a
MiliA, 40 μM, 1d
0% 2% 7%
5% 40% 25%
0% 2% 7%
0% 2% 7%
1% 1% 5%
1% 1% 5%
0% 1% 6%
4% 41% 17%
Propidium Iodide
Annexin V
D
PC-12
MiliA, 40 μM, 3d
1% 0% 2%
4% 5% 11%
PFTα
0% 1% 6%
1% 2% 6%
zVAD (20 μM) + PFTα (50 μM)
1% 2% 3%
1% 2% 4%
zVAD (20 μM)
0% 1% 4%
4% 6% 11%
Propidium Iodide
Annexin V

◀ **Fig. 7** MiliA-dependent Apoptosis and nuclear translocation of AIF is blocked by PFTα, an inhibitor of p53 transcriptional activity. 50 μM PFTα, 20 μM zVAD or PFTα and 20 μM zVAD were added 30 min prior to the administration of 40 μM MiliA. (**a**, **c**) N2a and PC-12 cells were incubated with 50 μM PFTα prior to addition of 40 μM MiliA or vehicle only for 6 h (N2a) and 3 days (PC-12), respectively. The cells were subsequently fixed, stained and analysed for AIF localisation (green) by immunofluorescence microscopy. The DNA was counterstained using Dapi (shown in blue). (**b**, **d**) FACS analysis of Annexin V/PI double stained cells revealed a clear reduction of Annexin V- and Annexin V/PI-positive N2a (**b**) or PC-12 (**d**) cells when co-treated with PFTα or PFTα/zVAD plus MiliA for one (N2a) and 3 days (PC-12), respectively. Addition of zVAD alone prior to MiliA-treatment only resulted in a minor reduction of Annexin V-positive cells

positively regulated by basal levels of p53 [16]. N2a showed higher basal levels of p53 and AIF and underwent apoptosis within a few hours whereas PC-12 had a low p53-expression and first reacted with up-regulation of protein-levels before execution of programmed cell death. In the course of MiliA-induced signalling we found additional phosphorylation of p53 at Ser15, which is essential for its pro-apoptotic function [40, 41]. Using PFTα, a compound that does not inhibit p53 phosphorylation but its transcriptional activity, abolished MiliA-dependent AIF translocation and initiation of apoptosis. This suggests that p53 was involved in regulation of AIF-expression and localisation.

However, these pathways described are not independent but interact with each other. Whereas inhibition of ERK1/2-signalling by the MEK-inhibitor UO126 had not specific effect (data not shown), blocking of the PI3-K/PKB pathway by LY294.002 suppressed MiliA-dependent early execution of apoptosis in N2a cells. This finding is in contrast to reports showing that inhibition of PI3-K would lead to stabilisation of p53 and facilitated induction of apoptosis [17, 49]: rather on the contrary, basal expression as well as phosphorylation at Ser15 were moderately repressed. It is, however, in agreement with reports that showed inhibition of cisplatin-induced, p53-dependent apoptosis by LY294.002 [39]. Although the PI3-K/PKB-pathway is mainly known for its pro-survival activity [50], it contributes in this complex context to apoptosis-induction. Additionally, it postponed MiliA-dependent AP-1 DNA-binding activity.

A differentiated phenotype in N2a cells could not be observed, which is likely due to the inhibition of PKB-derived signalling. Unfortunately, this assumption could not be verified in PC-12 cells as they fatally reacted to PI3-K-inhibition as described.

It seems clear that the two cell-lines undergo apoptosis through the same mechanisms once they are activated to a similar extent. Further, it seems to be clear that MiliA-dependent ROS-production does not play a decisive role as

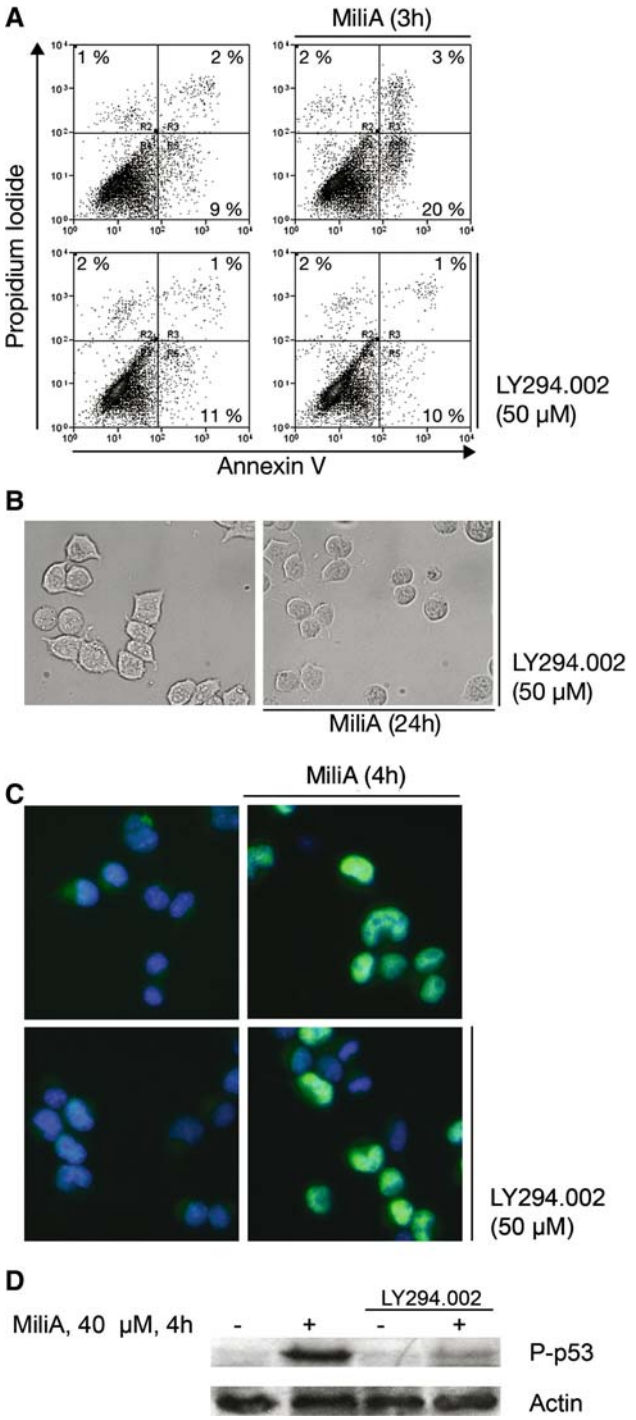

Fig. 8 Inhibition of PI3-K by LY294.002 blocks immediate onset of apoptosis in N2a cells and partly phosphorylation of p53 at Ser15. (**a**) Co-treatment with 40 μM MiliA (3 h) and 50 μM LY294.002 led to clearly reduced surface binding of Annexin V compared to the vehicle-treated controls. (**b**) LY294.002 efficiently inhibited late onset of cell death in N2a induced by 40 μM MiliA. (**c**, **d**) There was incomplete but significant reduction in p53 phosphorylation in LY294.002 and MiliA co-treated N2a cells after 4 h as shown by immunofluorescence microscopy (**c**) and SDS-PAGE (**d**)

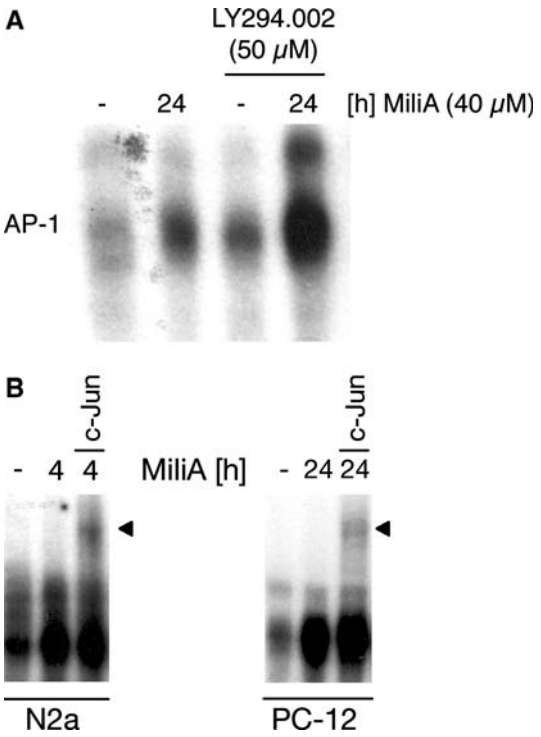

Fig. 9 LY294.002-dependent survival of MiliA-treated N2a cells leads to postponed AP-1 DNA-binding activity. (**a**) AP-1 DNA-binding activity occurs 24 h post-treatment in presence of LY294.002. (**b**) Binding of c-Jun to the AP-1 consensus sequence occurred both in N2a and PC-12 cells due to MiliA administration as visualised by supershift assays

both showed almost identical ROS-up-regulation. We nevertheless assume that it was involved to a certain degree. ROS also act as secondary messengers in intracellular signal transduction and help to induce or maintain the oncogenic phenotype of cancer cells [51]. Treatment with MiliA may just have driven the delicate balance over the edge. Preliminary data suggest that MiliA-treated primary cells (bovine lymph node cells and murine bone marrow mast cells) did not undergo cellular death even after a week's incubation. All cancer or cancerous cell lines tested on the other hand (PC-12, N2a, IMR-32, Jurkat T-cells, *Theileria parva*-infected T-cells [52]) died between 8 and 72 h after start of treatment (P. Küenzi and M. Hamburger, unpublished results).

Conclusion

Militarinone A induces neurite extension in PC-12 cells by persistent activation of pathways that are also involved in NGF-mediated differentiation, namely the PI3-K/PKB and MEK/ERK pathways. The continuous activation of these pathways finally leads to up-regulation of p53, release of AIF from mitochondria, and activation of the c-Jun/AP-1 transcription factor that has also been described as a "killer on the transcriptional leash" [43]. Application of MiliA to N2a cells, however, resulted in rapid onset of apoptosis by nuclear translocation of AIF, activation of caspases and c-Jun/AP-1. The main difference between the two cell types was the basal expression of p53, being high in N2a and low in PC-12. MiliA induced further stabilisation and activation of p53 as well as p53-dependent release and nuclear translocation of AIF in PC-12, which eventually resulted in apoptosis. MiliA induced the self-same pathways in both cell lines, initially leading to diverse, but finally to identical results.

References

1. Blesch A (2006) Neurotrophic factors in neurodegeneration. Brain Pathol 16:295–303
2. Pollack SJ, Harper SJ (2002) Small molecule Trk receptor agonists and other neurotrophic factor mimetics. Curr Drug Targets CNS Neurol Disord 1:59–80
3. Riese U, Ziegler E, Hamburger M (2004) Militarinone A induces differentiation in PC12 cells via MAP and Akt kinase signal transduction pathways. FEBS Lett 577:455–459
4. Frebel K, Wiese S (2006) Signalling molecules essential for neuronal survival and differentiation. Biochem Soc Trans 34:1287–1290
5. Vaudry D, Stork PJS, Lazarovici P, Eiden LE (2002) Differentiation pathway in PC12 Cells. Sci. STKE. http://stke.sciencemag.org/cgi/cm/stkecm;CMP_8038
6. Philpott KL, McCarthy MJ, Klippel A, Rubin LL (1997) Activated phosphatidylinositol 3-kinase and Akt kinase promote survival of superior cervical neurons. J Cell Biol 139:809–815
7. Kimura K, Hattori S, Kabuyama Y et al (1994) Neurite outgrowth of PC12 cells is suppressed by wortmannin, a specific inhibitor of phosphatidylinositol 3-kinase. J Biol Chem 269:18961–18967
8. Rubinfeld H, Seger R (2005) The ERK cascade: a prototype of MAPK signaling. Mol Biotechnol 31:151–174
9. Kimmelman AC, Nunez Rodriguez N, Chan AM (2002) R-Ras3/M-Ras induces neuronal differentiation of PC12 cells through cell-type-specific activation of the mitogen-activated protein kinase cascade. Mol Cell Biol 22:5946–5961
10. Modjtahedi N, Giordanetto F, Madeo F, Kroemer G (2006) Apoptosis-inducing factor: vital and lethal. Trends Cell Biol 16:264–272
11. Porter AG, Urbano AG (2006) Does apoptosis-inducing factor (AIF) have both life and death functions in cells? Bioessays 28:834–843
12. Cregan SP, Dawson VL, Slack RS (2004) Role of AIF in caspase-dependent and caspase-independent cell death. Oncogene 23:2785–2796
13. Cande C, Cohen I, Daugas E et al (2002) Apoptosis-inducing factor (AIF): a novel caspase-independent death effector released from mitochondria. Biochimie 84:215–222
14. Leist M, Jaattela M (2001) Four deaths and a funeral: from caspases to alternative mechanisms. Nat Rev Mol Cell Biol 2:589–598
15. Urbano A, Lakshmanan U, Choo PH et al (2005) AIF suppresses chemical stress-induced apoptosis and maintains the transformed state of tumor cells. Embo J 24:2815–2826
16. Stambolsky P, Weisz L, Shats I et al (2006) Regulation of AIF expression by p53. Cell Death Differ 13:2140–2149

17. Mayo LD, Donner DB (2002) The PTEN, Mdm2, p53 tumor suppressor-oncoprotein network. Trends Biochem Sci 27:462–467
18. Wymann MP, Zvelebil M, Laffargue M (2003) Phosphoinositide 3-kinase signalling—which way to target? Trends Pharmacol Sci 24:366–376
19. Vousden KH, Lu X (2002) Live or let die: the cell's response to p53. Nat Rev Cancer 2:594–604
20. Hofseth LJ, Hussain SP, Harris CC (2004) p53: 25 years after its discovery. Trends Pharmacol Sci 25:177–181
21. Polyak K, Xia Y, Zweier JL, Kinzler KW, Vogelstein B (1997) A model for p53-induced apoptosis. Nature 389:300–305
22. D'Autreaux B, Toledano MB (2007) ROS as signalling molecules: mechanisms that generate specificity in ROS homeostasis. Nat Rev Mol Cell Biol 8:813–824
23. Gloire G, Legrand-Poels S, Piette J (2006) NF-kappaB activation by reactive oxygen species: fifteen years later. Biochem Pharmacol 72:1493–1505
24. Lyakhovich VV, Vavilin VA, Zenkov NK, Menshchikova EB (2006) Active defense under oxidative stress. The antioxidant responsive element. Biochemistry (Mosc) 71:962–974
25. Nel A, Xia T, Mädler L, Li N (2006) Toxic potential of materials at the nanolevel. Science 311:622–627
26. Hess J, Angel P, Schorpp-Kistner M (2004) AP-1 subunits: quarrel and harmony among siblings. J Cell Sci 117:5965–5973
27. Rossler OG, Steinmuller L, Giehl KM, Thiel G (2002) Role of c-Jun concentration in neuronal cell death. J Neurosci Res 70:655–664
28. Karin M, Lin A (2002) NF-kappaB at the crossroads of life and death. Nat Immunol 3:221–227
29. van Delft MF, Huang DC (2006) How the Bcl-2 family of proteins interact to regulate apoptosis. Cell Res 16:203–213
30. Kuenzi P, Schneider P, Dobbelaere DA (2003) *Theileria parva*-transformed T cells show enhanced resistance to Fas/Fas ligand-induced apoptosis. J Immunol 171:1224–1231
31. Heussler VT, Kuenzi P, Fraga F, Schwab RA, Hemmings BA, Dobbelaere DA (2001) The Akt/PKB pathway is constitutively activated in Theileria-transformed leucocytes, but does not directly control constitutive NF-kappaB activation. Cell Microbiol 3:537–550
32. Nguyen T, Sherratt PJ, Pickett CB (2003) Regulatory mechanisms controlling gene expression mediated by the antioxidant response element. Annu Rev Pharmacol Toxicol 43:233–260
33. Botteron C, Dobbelaere D (1998) AP-1 and ATF-2 are constitutively activated via the JNK pathway in *Theileria parva*-transformed T-cells. Biochem Biophys Res Commun 246:418–421
34. Greene LA, Tischler AS (1976) Establishment of a noradrenergic clonal line of rat adrenal pheochromocytoma cells which respond to nerve growth factor. Proc Natl Acad Sci USA 73:2424–2428
35. Gogvadze V, Orrenius S, Zhivotovsky B (2006) Multiple pathways of cytochrome c release from mitochondria in apoptosis. Biochim Biophys Acta 1757:639–647
36. Schmidt K, Gunther W, Stoyanova S, Schubert B, Li Z, Hamburger M (2002) Militarinone A, a neurotrophic pyridone alkaloid from *Paecilomyces militaris*. Org Lett 4:197–199
37. Ly JD, Grubb DR, Lawen A (2003) The mitochondrial membrane potential (deltapsi(m)) in apoptosis: an update. Apoptosis 8:115–128
38. Simon HU, Haj-Yehia A, Levi-Schaffer F (2000) Role of reactive oxygen species (ROS) in apoptosis induction. Apoptosis 5:415–418
39. Bar J, Lukaschuk N, Zalcenstein A, Wilder S, Seger R, Oren M (2005) The PI3K inhibitor LY294002 prevents p53 induction by DNA damage and attenuates chemotherapy-induced apoptosis. Cell Death Differ 12:1578–1587
40. Bouleau S, Parvu-Ferecatu I, Rodriguez-Enfedaque A et al (2007) Fibroblast growth factor 1 inhibits p53-dependent apoptosis in PC12 cells. Apoptosis 12:1377–1387
41. Nakanishi M, Ozaki T, Yamamoto H et al (2007) NFBD1/MDC1 associates with p53 and regulates its function at the crossroad between cell survival and death in response to DNA damage. J Biol Chem 282:22993–23004
42. Komarov PG, Komarova EA, Kondratov RV et al (1999) A chemical inhibitor of p53 that protects mice from the side effects of cancer therapy. Science 285:1733–1737
43. Franzoso G, Zazzeroni F, Papa S (2003) JNK: a killer on a transcriptional leash. Cell Death Differ 10:13–15
44. Lopez-Maderuelo MD, Fernandez-Renart M, Moratilla C, Renart J (2001) Opposite effects of the Hsp90 inhibitor Geldanamycin: induction of apoptosis in PC12, and differentiation in N2A cells. FEBS Lett 490:23–27
45. Cheng Y, Schneider B, Riese U, Schubert B, Li Z, Hamburger M (2006) (+)-*N*-Deoxymilitarinone A, a neuritogenic pyridone alkaloid from the insect pathogenic fungus *Paecilomyces farinosus*. J Nat Prod 69:436–438
46. Symons M, Takai Y (2001) Ras GTPases: singing in tune. Sci STKE 2001: PE1
47. Wennerberg K, Rossman KL, Der CJ (2005) The Ras superfamily at a glance. J Cell Sci 118:843–846
48. Xu J, Ji LD, Xu LH (2006) Lead-induced apoptosis in PC 12 cells: involvement of p53, Bcl-2 family and caspase-3. Toxicol Lett 166:160–167
49. Sabbatini P, McCormick F (1999) Phosphoinositide 3-OH kinase (PI3K) and PKB/Akt delay the onset of p53-mediated, transcriptionally dependent apoptosis. J Biol Chem 274:24263–24269
50. Song G, Ouyang G, Bao S (2005) The activation of Akt/PKB signaling pathway and cell survival. J Cell Mol Med 9:59–71
51. Valko M, Leibfritz D, Moncol J, Cronin MT, Mazur M, Telser J (2007) Free radicals and antioxidants in normal physiological functions and human disease. Int J Biochem Cell Biol 39:44–84
52. Dobbelaere DA, Kuenzi P (2004) The strategies of the Theileria parasite: a new twist in host-pathogen interactions. Curr Opin Immunol 16:524–530